MICROLOCAL ANALYSIS, SMOOTH FRAMES AND DENOISING IN FOURIER SPACE[*]

RYUICHI ASHINO[†], STEVEN J. DESJARDINS[‡], CHRISTOPHER HEIL[§],
MICHIHIRO NAGASE[¶], AND RÉMI VAILLANCOURT[‖]

Dedicated to Yoshinori KAMETAKA *on the occasion of his 60th birthday*

Abstract. Microlocal filtering is performed with adapted orthonormal multiwavelets and smooth frame multiwavelets, which are derived from several generators. The values of the wavelet coefficients of a function give a rough estimate of its microlocal content, as shown by an example. Multidirectional denoising of images is presented as the action of a pseudodifferential operator which is the product of directional diffusion equations.

Key words. microlocal analysis, smooth frames, wavelet frames, denoising

AMS subject classifications. 42C40, 32A45, 46F15

1. Introduction. Wavelets have proven to be useful decomposition tools in a wide variety of applications throughout mathematics, science, and engineering. For example, the still-image compression standard known as JPEG2000 includes a wavelet option and the next video compression standard, MPEG-4, will be entirely wavelet based.

Hyperfunctions, which were introduced by Sato [13] and extensively developed by the Kyoto school of mathematics, can be considered to be sums of boundary values of holomorphic functions defined in infinitesimal wedges. Hyperfunctions are powerful tools in several applications; for example, vortex sheets in two-dimensional fluid dynamics are a realization of one-dimensional hyperfunctions. Analytic continuation in domains of special forms plays a key role in the theory of hyperfunctions. Microlocal analysis plays an important role in the theory of hyperfunctions, partial differential operators, and many other areas. In this theory, one can define the product of distributions and discuss the partial regularity of multidimensional distributions with respect to any independent variable.

In this paper, we discuss some particular multiwavelet constructions which are suited for microlocal filtering. In particular, expansion of a function or signal in terms of these multiwavelet bases or tight frames gives a rough estimate of its microlocal content, revealing directions of analyticity. The resolution of these multiwavelets in any given direction of analyticity can be made as fine as desired, at the cost of increasing the multiplicity of the multiwavelet basis or frame. We discuss the numerical implementation of these filters and apply them to multidirectional denoising

[†]Mathematical Sciences, Osaka Kyoiku University, Kashiwara, Osaka 582-8582, Japan (`ashino@cc.osaka-kyoiku.ac.jp`).

[‡]Department of Mathematics and Statistics, University of Ottawa, Ottawa, ON, Canada K1N 6N5 (`desjards@mathstat.uottawa.ca`).

[§]School of Mathematics, Georgia Institute of Technology, Atlanta, Georgia 30332-0160 USA (`heil@math.gatech.edu`).

[¶]Department of Mathematics, Graduate School of Science, Osaka University, Toyonaka, 560-0043, Japan (`nagase@math.wani.osaka-u.ac.jp`).

[‖]Department of Mathematics and Statistics, University of Ottawa, Ottawa, ON, Canada K1N 6N5 (`remi@uottawa.ca`).
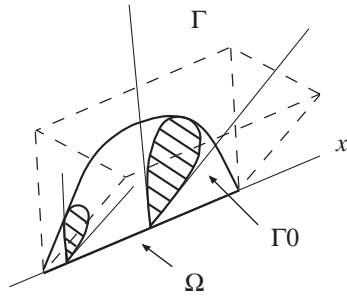
FIG. 2.1. *Infinitesimal wedge* $\Gamma 0$.

of two-dimensional images.

2. Microlocal Analysis. Our approach to microlocal analysis for Schwartz distributions is based on the theory of hyperfunctions, as introduced by Sato [13] and developed in [12] for the theory of linear partial differential equations with constant coefficients. A more complete treatment of microlocal filtering with multiwavelets can be found in [2]. Other treatments are found in [1] and [3]. A main goal is to find directions in which a function can be continued analytically for every point $x \in \mathbb{R}^n$.

2.1. Hyperfunctions in $\mathbb{R}^n$. A hyperfunction is defined as a sum of general boundary values of holomorphic functions in wedges whose edges are open subsets of $\mathbb{R}^n$. More precisely, a hyperfunction $f : \mathbb{R}^n \to \mathbb{C}$ is defined to be a sum

$$f(x) = \sum_{j=1}^{N} F_j(x + i\Gamma_j 0), \qquad x \in \Omega,$$

of boundary values

$$F_j(x + i\Gamma_j 0) = \lim_{\substack{y \to 0 \\ y \in \Gamma_j 0}} F_j(x + iy)$$

of holomorphic functions $F_j(z)$ in infinitesimal wedges $\Gamma_j 0$ with edge $\Omega \subset \mathbb{R}^n$ (see Fig. 2.1).

2.2. Microanalyticity. To characterize the microanalyticity of a tempered distribution $f \in \mathcal{S}'(\mathbb{R}^n)$ by its Fourier transform, $\widehat{f}$, we introduce the *dual cone*, Γ°, of Γ, defined by

$$\Gamma^\circ := \{\xi \in \mathbb{R}^n \,;\, y \cdot \xi \geq 0 \text{ for every } y \in \Gamma\}.$$

Figure 2.2 shows three examples of cones Γ, their dual cones Γ°, and their complements $(\Gamma^\circ)^c = \mathbb{R}^n \setminus \Gamma^\circ$.

LEMMA 2.1. *Let Γ be an open convex cone. A tempered distribution $f(x)$ can be represented as the limit $f(x + i\Gamma 0)$ of a slowly increasing holomorphic function $f(z)$ in the infinitesimal wedge $\mathbb{R}^n + i\Gamma 0$ if and only if the Fourier transform $\widehat{f}$ of f is exponentially decreasing in every closed proper subcone $\Gamma' \subset\subset (\Gamma^\circ)^c = \mathbb{R}^n \setminus \Gamma^\circ$.*

3. Microlocal Filtering. Given $f \in L^2(\mathbb{R}^n)$, let $f_{jk}(x)$ denote the scaled and shifted function

$$f_{jk}(x) = 2^{nj/2} f(2^j x - k), \qquad j \in \mathbb{Z}, \quad k \in \mathbb{Z}^n.$$
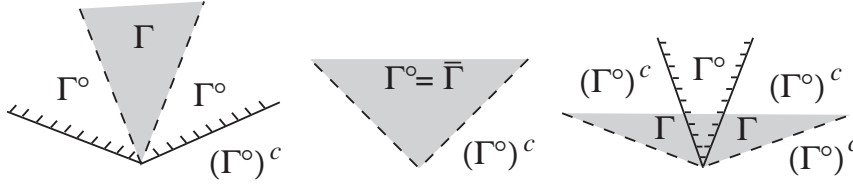
FIG. 2.2. *Open cone* Γ, *dual cone* Γ°, *and complement* $(\Gamma^\circ)^c$ *of dual cone.*

Let D be a finite index set with $\text{card}(D) = (2^n - 1)d$, $d \in \mathbb{N}$. A system

$$\{\psi_{jk}^\delta\}_{\delta \in D, j \in \mathbb{Z}, k \in \mathbb{Z}^n} \subset L^2(\mathbb{R}^n)$$

is called a *multiwavelet tight frame* with frame bound A, and in this case $\Psi = \{\psi^\delta\}_{\delta \in D}$ is called a set of *tight frame multiwavelets*, if

$$f = \frac{1}{A} \sum_{\substack{\delta \in D, \\ j \in \mathbb{Z}, k \in \mathbb{Z}^n}} \langle f, \psi_{jk}^\delta \rangle \, \psi_{jk}^\delta, \qquad \forall \, f \in L^2(\mathbb{R}^n). \tag{3.1}$$

If $\{\psi_{jk}^\delta\}_{\delta \in D, j \in \mathbb{Z}, k \in \mathbb{Z}^n} \subset L^2(\mathbb{R}^n)$ is an orthonormal basis for $L^2(\mathbb{R}^n)$ then it is called an *orthonormal multiwavelet basis*, and in this case $\Psi = \{\psi^\delta\}_{\delta \in D}$ is called a set of *orthonormal multiwavelets*.

Although a tight frame allows the basis-like representations in equation (3.1), a frame need not be an orthonormal or even independent sequence. Frames provide a useful model for obtaining signal decompositions in cases where redundancy, robustness, oversampling, and irregular sampling play a role. We refer to [4], [10], or [11] for basic information on frames and wavelets. It can be shown that Ψ is a set of orthonormal multiwavelets if and only if $\{\psi_{jk}^\delta\}_{\delta \in D, j \in \mathbb{Z}, k \in \mathbb{Z}^n}$ is a multiwavelet tight frame with frame bound $A = 1$ and $\|\psi^\delta\|_{L^2(\mathbb{R}^n)} = 1$ for $\delta \in D$.

Problems.
- Is it possible to construct orthonormal or tight frame multiwavelets $\Psi = \{\psi^\delta\}_{\delta \in D}$ corresponding to each microanalytic direction $\mathbb{S}^{n-1}$?
- Is it possible to obtain information on the microlocal content of $f \in L^2(\mathbb{R}^n)$ from the wavelet coefficients $\langle f, \psi_{jk}^\delta \rangle$?
- Can orthonormal or tight frame multiwavelet filtering separate microlocal contents?

We shall construct orthonormal multiwavelet bases or tight frames which enable us to obtain information on the microlocal content of signals or functions. As this separation of microlocal contents can be considered as a filtering operation, we call it *microlocal filtering*.

3.1. Orthonormal multiwavelets in $\mathbb{R}$. The one-dimensional case is summarized in the following theorem, where $[-2\pi, -4\pi]$ means $[-4\pi, -2\pi]$, and similarly later.

THEOREM 3.1. *Define $\psi^\pm$ by $\widehat{\psi^\pm} = \chi_{[\pm 2\pi, \pm 4\pi]}$ (Fig. 3.1). Then $\Psi := \{\psi^+, \psi^-\}$ is a set of orthonormal multiwavelets. Define the orthogonal projections $\mathcal{P}_\pm$ by*

$$\mathcal{P}_\pm f := \sum_{j,k \in \mathbb{Z}} \langle f, \psi_{jk}^\pm \rangle \, \psi_{jk}^\pm.$$
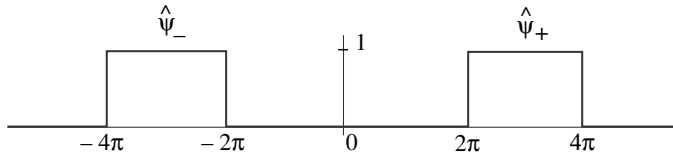
FIG. 3.1. *The Fourier transform of $\psi_\pm$.*

Then $\mathcal{P}_\pm f(x)$ can be extended analytically to $\{\operatorname{Im} z > 0\}$ and $\{\operatorname{Im} z < 0\}$, respectively.

Taken individually, $\psi^\pm$ generates an orthonormal wavelet basis for the classical Hardy space $H^2(\mathbb{R}_\pm)$ defined by

$$H^2(\mathbb{R}_\pm) = \left\{ f \in L^2(\mathbb{R}) \,;\, \widehat{f}(\xi) = 0 \quad \text{a.e. } \xi \leq (\geq)\, 0 \right\}.$$

This orthonormal multiwavelet basis was discussed in [5], and smooth tight multiwavelet frames were also constructed there (see also the discussion in [11, Section 8.4]). In the one-dimensional case, there are only two directions of analyticity, while in the n-dimensional case, the set of all microanalytic directions is $\mathbb{S}^{n-1}$, which is an infinite set. In Theorem 3.2, we will give a generalization of Theorem 3.1 to the n-dimensional case. An n-dimensional smooth multiwavelet tight frame will be given in Theorem 3.3. Using an expansion into these bases or frames, it is possible to tell fairly well in which directions f is microanalytic. The price for good angular resolution in $\mathbb{S}^{n-1}$ is the need for many multiwavelets.

3.2. Orthonormal multiwavelets in $\mathbb{R}^n$. The following notation will be used.
- $\eta = (\eta_1, \ldots, \eta_n) \in H := \{\pm 1\}^n$.
- $\varepsilon = (\varepsilon_1, \ldots, \varepsilon_n) \in E := \{0,1\}^n \setminus \{0\}, \quad j \in \mathbb{Z}_+$.
- $\varepsilon.* \eta := (\varepsilon_1\eta_1, \ldots, \varepsilon_n\eta_n)$.
- $\mathcal{Q}_{j,\varepsilon,\eta} := \left\{ \prod_{k=1}^n \left[\eta_k(\ell_k - 1), \eta_k\ell_k \right] + 2^j(\varepsilon.*\eta) : 1 \leq \ell_1, \ldots, \ell_n \leq 2^j, \ \ell_1, \ldots, \ell_n \in \mathbb{N} \right\}$.
- $2\pi\mathcal{Q}_{j,\varepsilon,\eta} := \{ 2\pi Q \,;\, Q \in \mathcal{Q}_{j,\varepsilon,\eta} \}$.
- $\mathbb{Z}_+^{E \times H}$ is the set of all functions from $E \times H$ to $\mathbb{Z}_+$.

THEOREM 3.2. *Fix $j \in \mathbb{Z}_+$, $\varepsilon \in E$, $\eta \in H$. For $Q \in \mathcal{Q}_{j,\varepsilon,\eta}$, define ψ_Q by*

$$\widehat{\psi}_Q = \chi_{2\pi Q},$$

where $\chi_{2\pi Q}$ is the characteristic function of the cube $2\pi Q$. For $\rho \in \mathbb{Z}_+^{E \times H}$, let

$$\mathcal{Q}_\rho := \bigcup_{(\varepsilon,\eta) \in E \times H} 2\pi\mathcal{Q}_{\rho(\varepsilon,\eta),\varepsilon,\eta}.$$

Then $\Psi := \{\psi_Q\}_{Q \in \mathcal{Q}_\rho}$ is a set of orthonormal multiwavelets.

Figure 3.2 illustrates the 2-D multiwavelets constructed in Theorem 3.2. Multiwavelets are masks in Fourier space — they are characteristic functions of cubes $2\pi Q$. The left part of Figure 3.2 shows 12 multiwavelet functions. For finer resolution in Fourier space, we need a greater number of multiwavelets. The right part of the Figure 3.2 shows 27 multiwavelet functions.

3.3. Smooth tight wavelet frames in $\mathbb{R}^n$. Smooth tight multiwavelet frames are obtained by convolving characteristic functions of cubes πQ so that the support
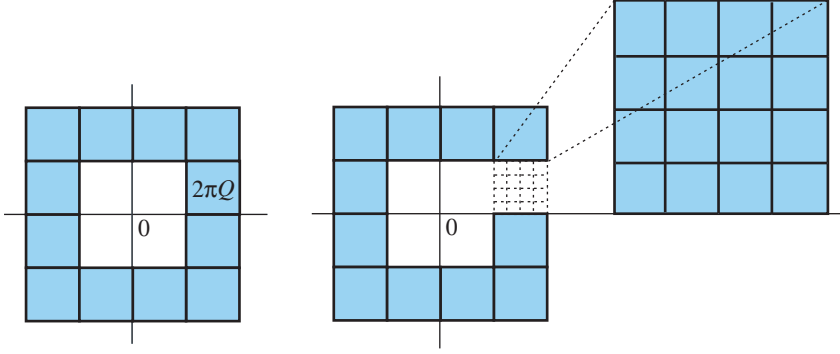
FIG. 3.2. *2-D orthonormal multiwavelet functions in Fourier space.*

of the smoothed functions have support inside cubes $2\pi Q$. This is achieved by considering the next inside annulus of cubes πQ in the left part of Fig. 3.2.

Let $\vartheta(t)$ be a $C_0^\infty(\mathbb{R})$-function of one variable satisfying

$$\vartheta(t) \geq 0, \qquad \vartheta(t) = \vartheta(-t), \qquad \int_{\mathbb{R}} \vartheta(t)\, dt = 1, \qquad \vartheta(t) = \begin{cases} 1, & |t| \leq \frac{1}{3}; \\ 0, & |t| \geq \frac{2}{3}. \end{cases}$$

For $\alpha > 0$ and $\xi = (\xi_1, \xi_2, \ldots, \xi_n) \in \mathbb{R}^n$, let

$$\vartheta_\alpha(\xi) = \frac{1}{\alpha^n} \prod_{j=1}^n \vartheta\left(\frac{\xi_j}{\alpha}\right).$$

THEOREM 3.3. *Fix $j \in \mathbb{Z}_+$, $\varepsilon \in E$, $\eta \in H$, and $\alpha \in (0, 1/2)$. Define*

$$\lambda_Q(\xi) := (\vartheta_\alpha * \chi_{\pi Q})(\xi) = \int_{\mathbb{R}^n} \vartheta_\alpha(\xi - \zeta)\, \chi_{\pi Q}(\zeta)\, d\zeta, \qquad Q \in \mathcal{Q}_{j,\varepsilon,\eta},$$

where $\chi_{\pi Q}$ is the characteristic function of the cube πQ. For $\rho \in \mathbb{Z}_+^{E \times H}$, let

$$\widetilde{\mathcal{Q}}_\rho := \bigcup_{(\varepsilon,\eta) \in E \times H} \pi \mathcal{Q}_{\rho(\varepsilon,\eta),\varepsilon,\eta}, \qquad \tau_\rho(\xi) := \sum_{j \in \mathbb{Z}, Q \in \widetilde{\mathcal{Q}}_\rho} |\lambda_Q(2^j \xi)|^2,$$

and, for $Q \in \widetilde{\mathcal{Q}}_\rho$, define $\psi_Q(x)$ by

$$\widehat{\psi}_Q(\xi) := \tau_\rho(\xi)^{-1/2}\, \lambda_Q(\xi).$$

Then $\Psi := \{\psi_Q\}_{Q \in \widetilde{\mathcal{Q}}_\rho}$ is a set of tight frame multiwavelets.

Theorem 3.3 follows from Theorem 3.4, which is essentially [9, Theorem 1].

THEOREM 3.4. $\Psi = \{\psi^\delta\}_{\delta \in D}$ *is a set of tight frame multiwavelets with frame bound $A = 1$ if and only if the following two equalities are satisfied:*

$$\sum_{\substack{\delta \in D \\ j \in \mathbb{Z}}} |\widehat{\psi^\delta}(2^j \xi)|^2 = 1, \qquad a.e.\ \xi \in \mathbb{R}^n, \tag{3.2}$$
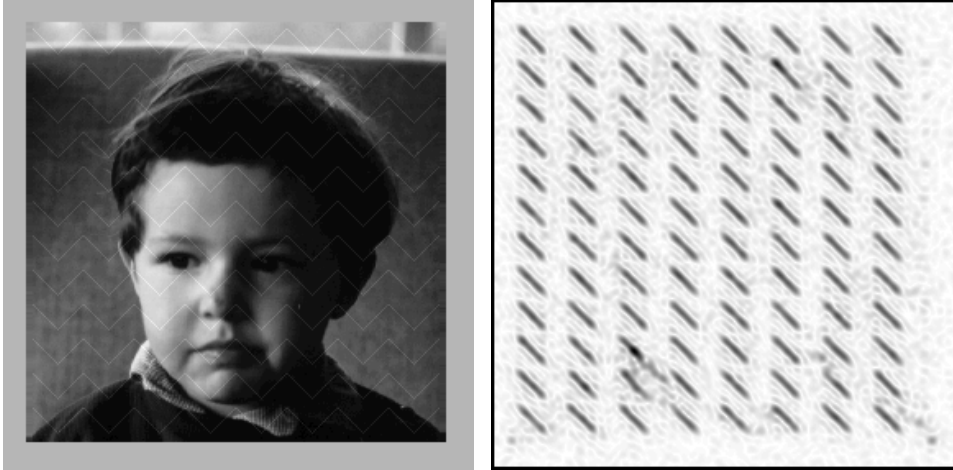
FIG. 4.1. *Left: Positive figure of boy behind an almost invisible zigzag grid. Right: Negative figure localizing the zigzag grid downward singularities.*

and

$$t_q(\xi) = 0, \qquad a.e.\ \xi \in \mathbb{R}^n,\ \forall\, q \in \mathbb{Z}^n \backslash (2\mathbb{Z})^n, \tag{3.3}$$

where

$$t_q(\xi) := \sum_{\substack{\delta \in D \\ j \in \mathbb{Z}_+}} \widehat{\psi^\delta}(2^j \xi)\, \overline{\widehat{\psi^\delta}(2^j(\xi + 2\pi q))}, \qquad \mathbb{Z}_+ := \mathbb{N} \cup \{0\}. \tag{3.4}$$

Note that $q \in \mathbb{Z}^n \backslash (2\mathbb{Z})^n$ means that at least one component q_j of q is an odd integer.

4. Numerical applications. Smooth frame wavelets $\{\psi_{j,k}^\ell\}$ can locate the singularity of a figure f by filtering $\widehat{f}$ away from the origin, since singularities are associated with high frequencies. Numerically, figures are discretized over rectangular matrices. In the left part of Fig. 4.1, the boy is shown behind a fine zigzag grid. Since the smooth filters consisting of tapered characteristic functions of squares cover a 287×287 matrix [6], the boy image is embedded into the central part of a 287×287 matrix.

The smooth filters consist of tapered characteristic functions of squares covering a 287×287 matrix. By filtering along the secondary diagonal with a smooth frame wavelet with support in the upper right corner of $\widehat{f}$, at a right angle with the downward parts of the grid, these downward parts are localized by means of the frame coefficients

$$\langle f, \psi_{j,k}^\ell \rangle = \frac{1}{2\pi} \langle \widehat{f}, \widehat{\psi}_{j,k}^\ell \rangle,$$

as can be seen in the right part of Fig. 4.1. The upward parts of the grid can be localized by filtering along the main diagonal in the upper left corner of $\widehat{f}$.

4.1. Multidirectional denoising. Multidirectional filtering by a product filter [7] consists in applying the one-dimensional diffusion operator in several directions

with a small step size in Fourier space. This operation removes some random and Gaussian noise without oversmearing edges. Once the filter is constructed for images of a given size, its application on a sequence of noisy images of the same size is very fast.

Diffusion in the x-direction is governed by $u_t = u_{xx}$, in the y-direction by $u_t = u_{yy}$. To diffuse in the direction of a line that makes an angle of θ with the x-axis, the governing equation is

$$u_t = \cos^2 \theta \, u_{xx} + 2 \sin \theta \cos \theta \, u_{xy} + \sin^2 \theta \, u_{yy}.$$

Applying the two-dimensional Fourier transform

$$\widehat{u}(\xi, \eta) = \int_{-\infty}^{\infty} \int_{-\infty}^{\infty} u(x, y) \, e^{-i(\xi x + \eta y)} \, dx \, dy.$$

to the diffusion equation, we obtain the equation

$$\begin{aligned} \widehat{u}_t &= -\xi^2 \cos^2 \theta \, \widehat{u} - 2\,\xi\,\eta\,\sin\theta\cos\theta\,\widehat{u} - \eta^2 \sin^2 \theta \, \widehat{u} \\ &= -[\xi \cos \theta + \eta \sin \theta]^2 \, \widehat{u}, \end{aligned}$$

whose solution is

$$\widehat{u}(\xi, \eta, t) = \widehat{u}(\xi, \eta, 0) \, \exp(-[\xi \cos \theta + \eta \sin \theta]^2 \, t).$$

One can diffuse noise in many directions, specified by angles θ_k, by means of the equation

$$u_t = \sum_k [\cos^2 \theta_k \, u_{xx} + 2 \sin \theta_k \cos \theta_k \, u_{xy} + \sin^2 \theta_k \, u_{yy}].$$

In the Fourier domain, this equation becomes

$$\widehat{u}_t = -\left(\sum_k [\xi \cos \theta_k + \eta \sin \theta_k]^2 \right) \widehat{u},$$

with solution

$$\widehat{u}(\xi, \eta, t) = \widehat{u}(\xi, \eta, 0) \, \exp\left(-\sum_k [\xi \cos \theta_k + \eta \sin \theta_k]^2 \, t \right) := \widehat{u}(\xi, \eta, 0) \, g(\xi, \eta, t).$$

The denoised image is given by the pseudodifferential operator

$$u(x, y, t) = \frac{1}{(2\pi)^2} \int_{-\infty}^{\infty} \int_{-\infty}^{\infty} e^{i(\xi x + \eta y)} \, g(\xi, \eta, t) \, \widehat{u}(\xi, \eta, 0) \, d\xi \, d\eta.$$

Therefore, if $\widehat{u}(\xi, \eta, 0)$ is the Fourier transform of a noisy image, then applying the multidirectional operator in the Fourier domain reduces to matrix multiplication with an appropriately chosen value of t.

Signal-to-noise ratio (SNR) is defined by the formula

$$\text{SNR} = \frac{\sum_{i=1}^{m} \sum_{j=1}^{n} u(i,j)^2}{\sum_{i=1}^{m} \sum_{j=1}^{n} [u(i,j) - U(i,j)]^2} = \frac{\|u\|_F^2}{\|u - U\|_F^2}, \tag{4.1}$$
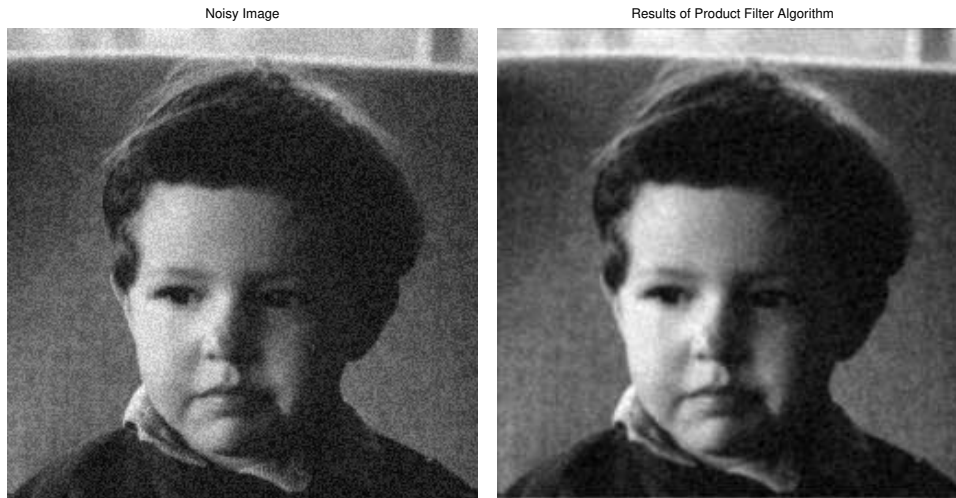
FIG. 4.2. *Left: Noisy figure with SNR = 12.7213. Right: Denoised image with SNR = 15.5816.*

where $[u(i,j)]$ and $[U(i,j)]$ represent the original and noisy images, respectively, as matrices and $\| \cdot \|_F$ is the Frobenius matrix norm. Ideally, if noise were perfectly removed from a noisy image, the result would be $u = U$ and SNR is infinite. In general, a higher SNR value signifies a better result, though visual observation is the true measurement, as two matrices may have the same norm and yet appear completely different when viewed as images.

The boy figure with added random noise of intensity 50, with signal to noise ratio SNR = 12.7213, is shown in the left part of Fig 4.2. This noisy image is denoised with the multidirectional filter with 256 directions and $t = 0.0003$. The result, with SNR = 15.5816, is shown in the right part of Fig 4.2.

REFERENCES

[1] R. Ashino, C. Heil, M. Nagase, and R. Vaillancourt, *Microlocal analysis and multiwavelets*, in Geometry, Analysis and Applications (Varanasi, 2000), 293–302, R. S. Pathak, ed., World Scientific, River Edge, NJ, 2001.

[2] R. Ashino, C. Heil, M. Nagase, and R. Vaillancourt, *Microlocal filtering with multiwavelets*, Comput. Math. Appl., **41** (2001), pp. 111–133.

[3] R. Ashino, C. Heil, M. Nagase, and R. Vaillancourt, *Multiwavelets, pseudodifferential operators and microlocal analysis*, in Wavelet Analysis and Applications, D. Deng, D. Huang, R.-Q. Jia, and W. Lin eds., AMS/IP Studies in Advanced Mathematics, Vol. 25, American Mathematical Society, Providence, RI, 2002.

[4] I. Daubechies, *Ten Lectures on Wavelets*, SIAM, Philadelphia, 1992.

[5] I. Daubechies, A. Grossmann, and Y. Meyer, *Painless nonorthogonal expansions*, J. Math. Phys., **27**(5) (1986), pp. 1271–1283.

[6] S. J. Desjardins, *Image Analyis in Fourier space*, Doctoral dissertation, University of Ottawa, Ottawa, Ontario, Canada (submitted).

[7] S. J. Desjardins and R. Vaillancourt, *Image de-noising by a multi-directional diffusion equation*, Mathematical Reports Acad. Sci. Canada, to appear.

[8] L. Alvarez, P.-L. Lions, and J.-M. Morel, *Image selective smoothing and edge detection by nonlinear diffusion. II*, SIAM J. Numer. Anal., **26**(3) (1992), pp. 845–866.

[9] M. Frazier, G. Garrigós, K. Wang, and G. Weiss, *A characterization of functions that generate wavelet and related expansion*, J. Fourier Anal. Appl. **3** (1997), Special Issue, pp. 883–906.

[10] C. E. Heil and D. F. Walnut, *Continuous and discrete wavelet transforms*, SIAM Review, **31**(4) (1989), pp. 628–666.

[11] E. Hernández and G. Weiss, *A First Course on Wavelets*, CRC Press, Boca Raton, FL, 1996, Chapter 7 and 8.
[12] A. Kaneko, *Linear Partial Differential Equations with Constant Coefficients*, Iwanami, Tokyo, 1992. (Japanese)
[13] M. Sato, *Theory of hyperfunctions I*, J. Fac. Sci. Univ. Tokyo, Sec. I, **8**(1) (1959), pp. 139–193.